Frontiers of Information Technology & Electronic Engineering
www.jzus.zju.edu.cn; engineering.cae.cn; www.springerlink.com
ISSN 2095-9184 (print); ISSN 2095-9230 (online)
E-mail: jzus@zju.edu.cn

Dynamic modeling of a wave glider*

Chun-lin ZHOU†, Bo-xing WANG, Hong-xiang ZHOU, Jing-lan LI, Rong XIONG†‡

(*College of Control Science and Engineering, Zhejiang University, Hangzhou 310027, China*)

†E-mail: c_zhou@zju.edu.cn; rxiong@zju.edu.cn

Received May 3, 2017; Revision accepted Aug. 23, 2017; Crosschecked Sept. 27, 2017

Abstract: We propose a method to establish a dynamic model for a wave glider, a wave-propelled sea surface vehicle that can make use of wave energy to obtain thrust. The vehicle, composed of a surface float and a submerged glider in sea water, is regarded as a two-particle system. Kane's equations are used to establish the dynamic model. To verify the model, the design of a testing prototype is proposed and pool trials are conducted. The speeds of the vehicle under different sea conditions can be computed using the model, which is verified by pool trials. The optimal structure parameters useful for vehicle designs can also be obtained from the model. We illustrate how to build an analytical dynamics model for the wave glider, which is a crucial basis for the vehicle's motion control. The dynamics model also provides foundations for an off-line simulation of vehicle performance and the optimization of its mechanical designs.

Key words: Wave-propelled vehicle; Dynamic modeling; Sea surface vehicle; Wave glider
https://doi.org/10.1631/FITEE.1700294 **CLC number:** TP242

1 Introduction

Oceanographic research and marine environment monitoring missions are performed generally by way of traditional platforms such as ships, buoys, satellites, moorings, and autonomous underwater vehicles (AUVs). These platforms usually depend on traditional energy such as gas or electricity. Future marine research demands an autonomous platform that can withstand a persistent and long-distance ocean exploration (Wiggins *et al.*, 2010; Liu *et al.*, 2011; Carragher *et al.*, 2013). Marine robots have been modified to use environment resources for propulsion instead of traditional propellers or motors (Manley and Willcox, 2010). The wave-propelled autonomous surface vehicle can harvest wave energy for propulsion mechanically and persistently without any traditional energy supplies. The wave-propelled autonomous surface vehicle, also called the 'wave glider' (Hine *et al.*, 2009; Manley and Hine, 2016), consists of a submerged glider and a surface float. The two parts are connected by a flexible cable. The vehicle can obtain propulsion by converting vertical ocean wave energy into forward moving energy. Its motion can be divided into a rising process and a sinking process (Fig. 1). During the rising process, the submerged glider in deeper and calmer water is pulled up by the rising float which moves upwards consistently as the rising wave. During this process, wings on the glider are forced to rotate downwards as the water generates a positive angle of attack, producing a forward propulsion and drags the surface float to move forward. During the sinking process, water forces the wings to rotate upward as the glider sinks. In this case, drag force F_g also has a forward component, and forward propulsion can be produced. The birth of the wave glider brings an exciting future for long-distance ocean exploration without fuel supply. However, there still exist challenges in the application of such vehicles. To

‡ Corresponding author

* Project supported by the National Natural Science Foundation of China (Nos. 51305396 and U1509210) and the Fundamental Research Funds for the Central Universities, China

Chun-lin ZHOU, http://orcid.org/0000-0001-6939-9732

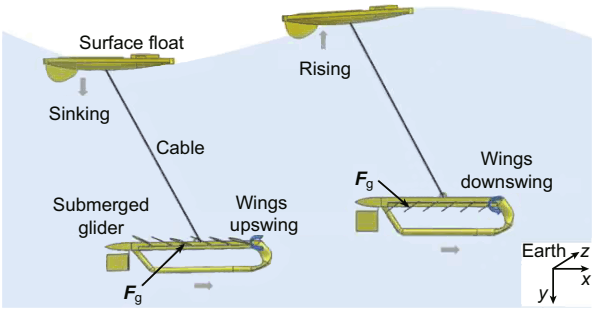

Fig. 1 Motion principle of the wave-propelled vehicle

control the motion of the wave glider, its forward speed must either have a known value or can be predicted (Cameron, 1994; Lolla *et al.*, 2012), because current methods in motion control and path planning for mobile robots are all based on a known speed. However, this foundation does not exist for the wave glider (Ngo *et al.*, 2013). The wave glider obtains its speed in a passive manner depending on the real-time up-down motion of ocean waves, which is impossible to control. Therefore, it is important to use a dynamics model to predict the speed of the wave glider according to ocean wave conditions.

The forward speed of the wave-propelled vehicle is determined mainly by both its mechanisms and environmental factors, which are dominated by wave height and period. It is generally known that there are two methods for solving such problems: the mechanism modeling method (Caiti *et al.*, 2011; Song *et al.*, 2016) and the regression analysis method based on experimental data (Ngo *et al.*, 2013). Smith *et al.* (2011) presented the formulation of a linear regression model with the least-squares solution to predict the vehicle speed in the desired direction, given the wave height, ocean currents, wind velocity, and direction. They pointed out that the significant factors are wave height and period. Later, Ngo *et al.* (2014) turned to the Gaussian process model, which can predict the speed at the desired location and time by using forecasted environmental parameters after training with data on historical vehicle speeds and environmental parameters. The precision of prediction by regression analysis methods depends greatly on large-scale training data and their representations. It is difficult to collect the training data that cover various time and locations, as the ocean environment varies temporally and spatially. The trained model may therefore be unsuitable for application to another vehicle with different mechanical parameters.

Based on analysis of the mechanism, the dynamic model can determine the forward speed of the vehicle theoretically by incorporating environmental parameters, and be employed to optimize the mechanism parameters of the vehicle and to aid in navigation. Kraus and Bingham (2011) developed a 2D simplified dynamic model in the vertical plane using Newton's law for control and estimation. However, there is no analysis of the dynamics of the model under different sea states, and it is not suitable for real-time prediction. The wave-propelled vehicle is such a new class of two-body surface vehicle that there is limited research on it, especially on the modeling that is different from the traditional single-body autonomous surface vehicles (ASVs) or gliders.

A dynamic model that incorporates vehicle speed and sea conditions is of great value for motion control. By using such a model, one can predict the vehicle speed according to ocean forecast data to provide a foundation for path planning and navigation. With the aim of predicting the speed of the vehicle and optimizing its mechanism parameters for further applications, we will establish a dynamic model of the vehicle, with which we can provide a method for incorporating environmental parameters into the model, and determine the forward speed of the vehicle consequently. The vehicle can move in two ways: one way is by obtaining thrust from the wave up-down motion, which is the focus of this study; the other is the vehicle drifting motion as sea water flows. The latter is irrelevant to the dynamic model discussed in this study. Our dynamic model is based upon significant wave height and period, regardless of the impact of ocean flow, as carried out by Ngo *et al.* (2014).

2 Dynamic model

To predict the forward speed under different sea states and to optimize the mechanism parameters of the vehicle, a dynamic model related to sea state is established. To simplify analysis, the heave motion of wave is assumed to be modeled as a sinusoidal function using the airy wave theory first. We can use the following equation to describe the heave motion

of wave approximately (Cong *et al.*, 2009):

$$y(x,t)=\frac{H}{2}\sin(kx-\omega t+\varepsilon), \tag{1}$$

where H is the wave height, ω is the wave frequency, $k=2\pi/\lambda$ is the sequence number of wave, λ is the wave length, and ε is the initial phase.

At a certain point where a surface vehicle runs, Eq. (1) becomes a vibration equation. The vehicle can be regarded as a particle moving with the wave. Kane's method is adopted to build the dynamic model as it is an elegant and effective means to develop the dynamic equations for multi-body systems (Ma *et al.*, 1988; Tarn *et al.*, 1996). With the motion principle described in Section 1, we can infer that the ocean state has a direct effect on the motion of the wave-propelled vehicle, apart from its mechanism parameters. The wave height and period are the dominant environmental factors for the forward speed of the vehicle.

The general brief procedure for Kane's method is: First, select generalized coordinates and speeds based on the degrees of freedom (DOFs) of the system; Second, generate the expressions for velocity, angular velocity, and acceleration of each body based on kinematic analysis; Third, calculate the system's generalized inertial force and generalized active force contributed by each body; Finally, obtain the system dynamic model using Kane's equation.

Before establishing the model, further analysis on the motion of the system and several simplification assumptions have to be made (Daugherty and Franzini, 1997):

1. When the only concern is the forward speed of the vehicle, its motion can be limited approximately to a 2D vertical plane. It is difficult to hold the glider and the surface float in a vertical plane. It can be realized only when the glider performs steering or there are turbulent flows in the sea water. In most cases, the vehicle performs straight movements. The glider and the float are all equipped with rudders to maintain their movement direction. These two rudders can effectively prevent the rotation around the y axis (yaw motion). Additionally, the cable tension ensures that the two rigid bodies are kept in the same vertical plane. Therefore, in terms of predicting the forward speed, the assumption can be held. The vehicle can be simplified to a 2-DOF system.

2. The weight of the glider is much larger than its buoyancy. It guarantees that the cable connecting the float and the glider is tightened. Therefore, the glider can always pull the float.

3. Two ends of the cable are tied at the center of gravity on the float and the glider. This hardware, together with the wing mechanism, ensures that there is no pitch motion when the glider swings with the motion of wave.

4. The surface float is designed to have enough surface area such that its heave motion is assumed to be consistent with the wave motion.

Because the cable connecting the float and the glider is kept tightened, the up-down motion of the whole system depends entirely on the sinusoidal wave motion. The rising and sinking motions are symmetrical. As a result, the dynamic models of the rising and sinking processes are similar. The difference between them lies in the fact that the wings downswing during the rising and sinking processes. It also results in different directional hydrodynamic forces on the wings. During the transient process between the two processes, the wings are in the state of angle adjustment, making no contribution to propulsion. The model for the rising process is developed as follows:

Step 1: The generalized speed is chosen if Kane's equations are applied. Since the forward speed of the surface float $v_{\mathrm{f},x}$ is a key variable of interest, it can be selected as a generalized speed $\dot{\pi}_1$. The speed of the glider $l\dot{\theta}$ seen from the surface float frame is taken as another generalized speed $\dot{\pi}_2$.

Step 2: Kinematic analysis is conducted and partial speeds are calculated. All notations used are shown in Fig. 2. We can construct the velocities of the float $\boldsymbol{v}_{\mathrm{f}}$ and the glider $\boldsymbol{v}_{\mathrm{g}}$ in the Earth reference frame as follows:

$$\begin{cases}\boldsymbol{v}_{\mathrm{f}}=v_{\mathrm{f},x}\cdot\boldsymbol{i}+v_{\mathrm{f},y}\cdot(-\boldsymbol{j}),\\ \boldsymbol{v}_{\mathrm{g}}=\boldsymbol{v}_{\mathrm{f}}+\boldsymbol{v}_l=v_{\mathrm{f},x}\cdot\boldsymbol{i}+v_{\mathrm{f},y}\cdot(-\boldsymbol{j})\\ \qquad\qquad +l\theta\cos\theta\cdot\boldsymbol{i}+l\theta\sin\theta\cdot(-\boldsymbol{j}),\end{cases} \tag{2}$$

where $\boldsymbol{i}$ and $\boldsymbol{j}$ are the unit vectors along the x-axis and y-axis, respectively. The accelerations of the float and the glider in the Earth reference frame can be derived from Eq. (2). The partial speeds of the float and the glider with respect to the generalized speeds $\dot{\pi}_1$ and $\dot{\pi}_2$ are

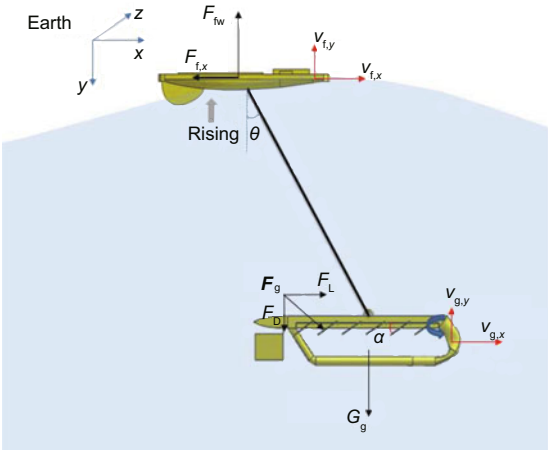

Fig. 2 Force analysis diagram

$$\begin{cases} \boldsymbol{u}'_{\mathrm{f},\dot{\pi}_1} = \partial \boldsymbol{v}_\mathrm{f}/\partial\dot{\pi}_1 = \boldsymbol{i}, \\ \boldsymbol{u}'_{\mathrm{f},\dot{\pi}_2} = \partial \boldsymbol{v}_\mathrm{f}/\partial\dot{\pi}_2 = \boldsymbol{0}, \\ \boldsymbol{u}'_{\mathrm{g},\dot{\pi}_1} = \partial \boldsymbol{v}_\mathrm{g}/\partial\dot{\pi}_1 = \boldsymbol{i}, \\ \boldsymbol{u}'_{\mathrm{g},\dot{\pi}_2} = \partial \boldsymbol{v}_\mathrm{g}/\partial\dot{\pi}_2 = \cos\theta\cdot\boldsymbol{i} + \sin\theta\cdot(-\boldsymbol{j}). \end{cases} \tag{3}$$

Step 3: The generalized active force and generalized inertial force are calculated. Force analysis should be implemented for both bodies before calculation. The active force on the glider consists of net gravity ($\boldsymbol{G}_\mathrm{g}$) and the hydrodynamic force on the wings ($\boldsymbol{F}_\mathrm{g}$). The active force on the float includes wave force $\boldsymbol{F}_\mathrm{fw}$ in the vertical direction and profile drag $\boldsymbol{F}_{\mathrm{f},x}$ along the direction of movement. They can be expressed as follows:

$$\boldsymbol{G}_\mathrm{g} = (m_\mathrm{g}g - \rho g V_\mathrm{g})\boldsymbol{j}, \tag{4}$$

where V_g and m_g are the volume and mass of the glider, respectively. $\boldsymbol{F}_\mathrm{g}$ can be expressed as

$$\boldsymbol{F}_\mathrm{g} = F_\mathrm{L}\boldsymbol{i} + F_\mathrm{D}\boldsymbol{j}, \tag{5}$$

where F_L and F_D are force components in horizontal and vertical directions, respectively (Fig. 2). The mold of $\boldsymbol{F}_\mathrm{g}$ can be expressed as

$$|\boldsymbol{F}_\mathrm{g}| = \frac{1}{2}\rho c S(v_{\mathrm{g},y}\cos\alpha - v_{\mathrm{g},x}\sin\alpha)^2, \tag{6}$$

where c is a drag coefficient, S is the total area of all wings, $v_{\mathrm{g},x}$ and $v_{\mathrm{g},y}$ are the velocity components of the glider in horizontal and vertical directions, respectively, and α is the angle of attack fixed by the mechanical hardware of the glider. The wings can rotate with the move of the glider. There are physical stoppers that limit the rotation range of the wings. The active force on the float is

$$\boldsymbol{F}_{\mathrm{f},x} = \frac{1}{2}\rho c S_\mathrm{f} v_{\mathrm{f},x}^2(-\boldsymbol{i}), \tag{7}$$

where S_f is the projection of the area of the float in the direction of motion. The wave force is

$$\boldsymbol{F}_\mathrm{fw} = -F_\mathrm{D}\boldsymbol{j} + m_\mathrm{f}\dot{\boldsymbol{v}}_{\mathrm{f},y} + m_\mathrm{g}\dot{\boldsymbol{v}}_{\mathrm{g},y}, \tag{8}$$

where m_f is the mass of the float. Generalized active force with respect to the generalized speeds $\dot{\pi}_1$ and $\dot{\pi}_2$ can be expressed as

$$\begin{cases} F_{\dot{\pi}_1} = (\boldsymbol{F}_{\mathrm{f},x} + \boldsymbol{F}_\mathrm{fw})\boldsymbol{u}'_{\mathrm{f},\dot{\pi}_1} + (\boldsymbol{G}_\mathrm{g} + \boldsymbol{F}_\mathrm{g})\boldsymbol{u}'_{\mathrm{g},\dot{\pi}_1}, \\ F_{\dot{\pi}_2} = (\boldsymbol{F}_{\mathrm{f},x} + \boldsymbol{F}_\mathrm{fw})\boldsymbol{u}'_{\mathrm{f},\dot{\pi}_2} + (\boldsymbol{G}_\mathrm{g} + \boldsymbol{F}_\mathrm{g})\boldsymbol{u}'_{\mathrm{g},\dot{\pi}_2}, \end{cases} \tag{9}$$

whose generalized inertial forces can be expressed as

$$\begin{cases} F^*_{\dot{\pi}_1} = -(m_\mathrm{f}\boldsymbol{a}_\mathrm{f}\boldsymbol{u}'_{\mathrm{f},\dot{\pi}_1} + m_\mathrm{g}\boldsymbol{a}_\mathrm{g}\boldsymbol{u}'_{\mathrm{g},\dot{\pi}_1}), \\ F^*_{\dot{\pi}_2} = -(m_\mathrm{f}\boldsymbol{a}_\mathrm{f}\boldsymbol{u}'_{\mathrm{f},\dot{\pi}_2} + m_\mathrm{g}\boldsymbol{a}_\mathrm{g}\boldsymbol{u}'_{\mathrm{g},\dot{\pi}_2}). \end{cases} \tag{10}$$

Step 4: According to Kane's equation:

$$F_\gamma + F^*_\gamma = 0, \tag{11}$$

where F_γ and F^*_γ are the generalized active force and inertial force with respect to the generalized speed, respectively. The dynamic model for the system can be derived by assembling Eq. (12) at the bottom of this page, where $v_{\mathrm{f},x}$ is the forward speed of the surface float and also seen as the forward speed of the vehicle. During the sinking process, nothing has to be modified but the direction of F_D. During the transient process, the wings adjust the angle of attack and make no contribution to propulsion; thus, it can be concluded that $\boldsymbol{F}_\mathrm{g} = \boldsymbol{0}$.

$$\begin{cases} \ddot{\theta} = \dfrac{-1}{m_\mathrm{g}l(m_\mathrm{f} + m_\mathrm{g}\sin^2\theta)}\{m_\mathrm{g}\cos\theta(F_L - F_{\mathrm{f},x} + m_\mathrm{g}l\dot{\theta}^2\sin\theta) - (m_\mathrm{f} + m_\mathrm{g}) \\ \quad \cdot[F_\mathrm{L}\cos\theta - (m_\mathrm{g}g - \rho g V_\mathrm{g} + F_\mathrm{D})\sin\theta - m_\mathrm{g}\dot{v}_{\mathrm{f},y}\sin\theta]\}, \\ \dot{v}_{\mathrm{f},x} = \dfrac{1}{m_\mathrm{f} + m_\mathrm{g}\sin^2\theta}[F_\mathrm{L}\sin^2\theta + (m_\mathrm{g}g - \rho g V_\mathrm{g} + F_\mathrm{D})\sin\theta\cos\theta + m_\mathrm{g}(\dot{v}_\mathrm{g}\sin\theta\cos\theta + l\dot{\theta}^2\sin\theta) - F_{\mathrm{f},x}]. \end{cases} \tag{12}$$

3 Simulation test of the dynamic model

Simulations have been conducted based on wave model (1) and dynamic model (12). The glider can obtain propulsion only when the ocean wave has sufficient heights, which are quantified by sea state levels. In practical applications, the wave glider usually runs under sea state levels 3–5. The parameters for the wave model, i.e., the data at different sea state levels, are given in Table 1. Parameters for model (12) are given in Table 2. These parameters are obtained from a lab testing prototype whose design will be presented in the next section. Here, we adopt its mechanical parameters for simulation. We are going to analyze the motion characteristic of the vehicle at various sea states through simulations. In the meantime, the feasibility of the model can be verified by simulation. Afterwards, the parameters of mechanism are optimized to improve the speed of the vehicle according to simulation results.

Table 1 Parameters of the wave at different sea state levels

Sea state level	H (m)	T (s)	ω (rad/s)
3	1.25	3.2	1.9635
4	2.50	4.0	1.5708
5	4.00	4.8	1.3090

Table 2 Parameters of the dynamic model

Parameter	Value	Parameter	Value
m_g	5 kg	c	0.8
m_f	2.2 kg	S	0.3 m^2
α	$\pi/4$	S_g	0.01 m^2
$\rho g V_g$	3.2 N	l	2 m

The heave motion of the float is assumed to be consistent with the wave motion as mentioned in Section 2. Taking sea state level 4 as an example, where the wave height is about 2.5 m and the wave period is about 4 s, the motion response curves can be derived from dynamic model (12) with suitable parameters using a numerical solution such as the Rugge-Kutta methods (Fig. 3). It can be seen that the speeds show a periodical pattern, which conforms to the motion of the ocean wave. The glider swings beneath the float. The positive angle values imply that the glider always pulls the float forward. The average forward speed (i.e., the traveling distance of the vehicle over one wave cycle) is about 0.81 m/s at sea state level 4.

To analyze the motion characteristics, several simulations are carried out at sea state levels 3, 4, and 5, respectively (Fig. 4). The average speeds are approximately 0.52, 0.81, and 1.06 m/s, respectively. For a given surface vehicle, the higher the sea level is, the faster the vehicle moves.

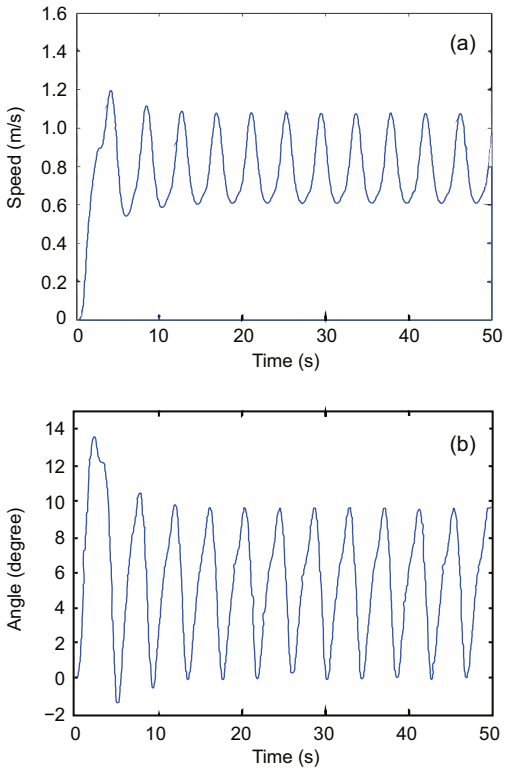

Fig. 3 Forward speed (a) and cable angle (b) of the vehicle at sea state level 4

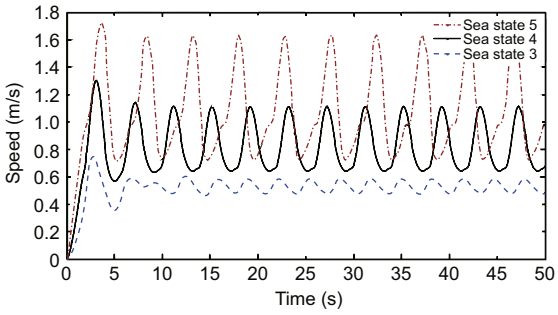

Fig. 4 Forward speeds at sea state levels 3, 4, and 5

The forward speed of the wave-propelled vehicle is determined mainly by both its mechanism parameters and environmental factors. In this part we discuss the influence of the key mechanism parameters on its speed. All the simulations are implemented at common sea state levels 3 and 4. The

forward speed curves under different lengths of cable are shown in Fig. 5. According to the speed curves, the optimal length is about 6 to 7 m, at which the speed becomes maximum. Fig. 6 shows that the maximum speed occurs when the angle of attack is about 20°–30°. The quality ratio of the submerged glider to the float has a positive correlation with the forward speed (Fig. 7), which can also be concluded naturally by the momentum conservation law. All these optimal key mechanism parameters are useful for the design of the vehicle (Zhou and Low, 2014).

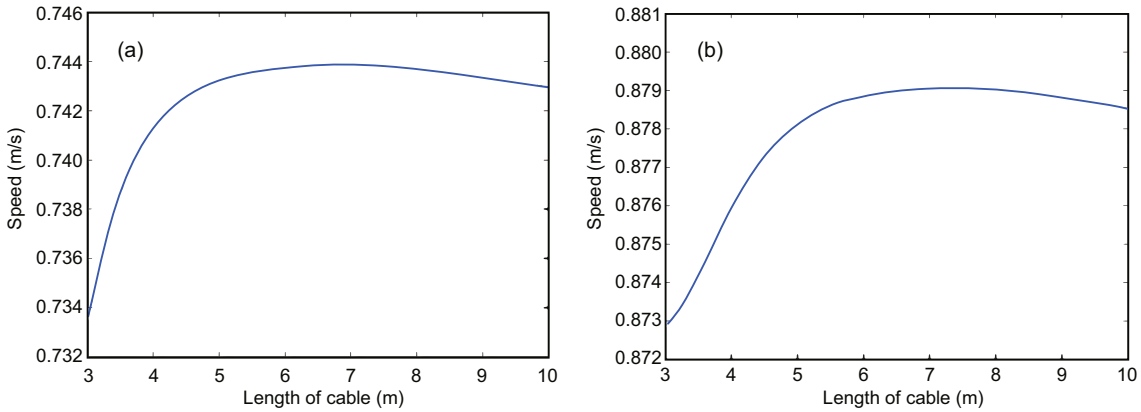

Fig. 5 Forward speed vs. length of cable under sea state levels 3 (a) and 4 (b)

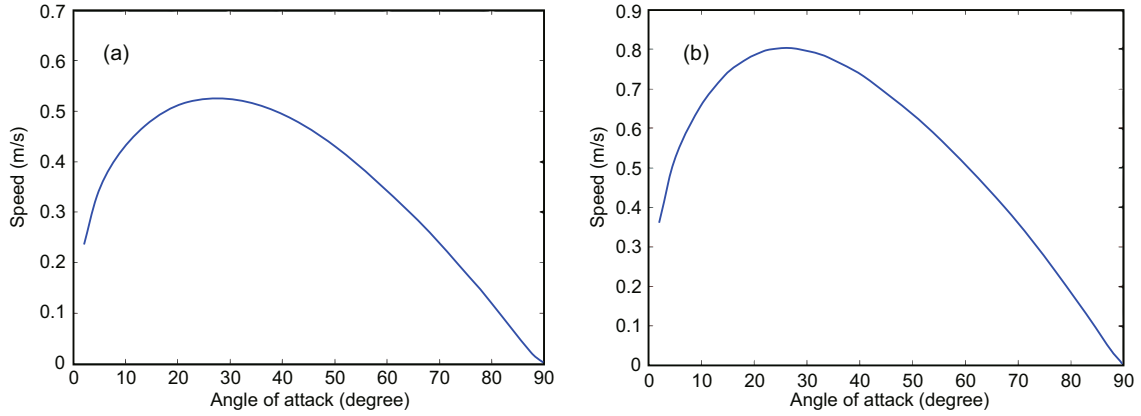

Fig. 6 Forward speed vs. angle of attack under sea state levels 3 (a) and 4 (b)

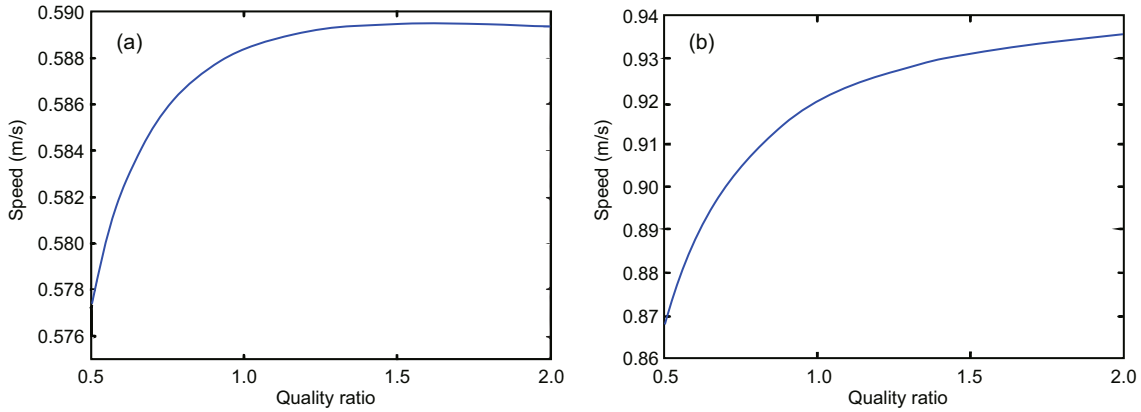

Fig. 7 Forward speed vs. quality ratio under sea state levels 3 (a) and 4 (b)

4 Pool trial exploration

It is inconvenient to conduct a test in real ocean conditions because of the complexity of the environment and the difficulties presented for data measurement. Instead, a test bed working in a pool is designed to verify the accuracy of the dynamic model and to further explore the motion principle of the wave-propelled vehicle. In this section, a brief introduction of the platform and its experimental procedure is given first. Then we discuss the experimental results by a qualitative comparison with the simulation results.

4.1 Setup of experiment

A pool testing prototype is developed to simulate the motion of the vehicle motivated by ocean waves. As depicted in Fig. 8, the surface float is simulated by a stage on linear guides. The glider is hung with a soft rope beneath the stage and works in water. A brushless servo motor (DC 24 V, 200 W) is used to generate the wave motion by pulling and releasing the glider periodically. Controlled by NI MyRIO^{TM} embedded hardware, the motor can produce motion profiles defined by Eq. (1). It pulls the glider upward to provide forward drag force for the stage. The rope is released when the glider drops down due to gravity and provides a down stroke forward force. In this manner, the stage can move under the drag from the submerged glider. A speed sensor (grating ruler) is adopted to monitor the real-time speed of the stage motion. The glider is equipped with four pairs of wings made from 1 mm thick stainless steel plates. All electronic devices are put on an aluminum plate that can slide freely on two parallel linear guides.

The whole test bed runs on an aluminum frame submerged in a lab water tank, as shown in Fig. 9. The motion process of the vehicle motivated by the up-and-down wave is simulated by the platform in which a motor is commanded to drag the glider up and down. Similarly, the simulated float is dragged forward by the glider. The forward speed of the float is acquired by the grating ruler attached to the frame. The dragged speed of the glider by the motor can be calculated by the rotation of the motor and the mean diameter of the lead screw. By this method, different sea state levels can be simulated by controlling the rotation speed of the motor. The impact of the angle of attack on the speed can be studied by adjusting the angle.

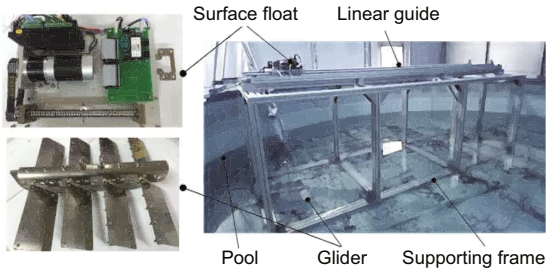

Fig. 9 Pool trial platform

4.2 Experiment results

In the experiments, the servo motor drives the lead screw. Rotation of the screw winds up the soft cable to pull up the glider. Once the glider reaches its highest position, the motor rotates inversely and the

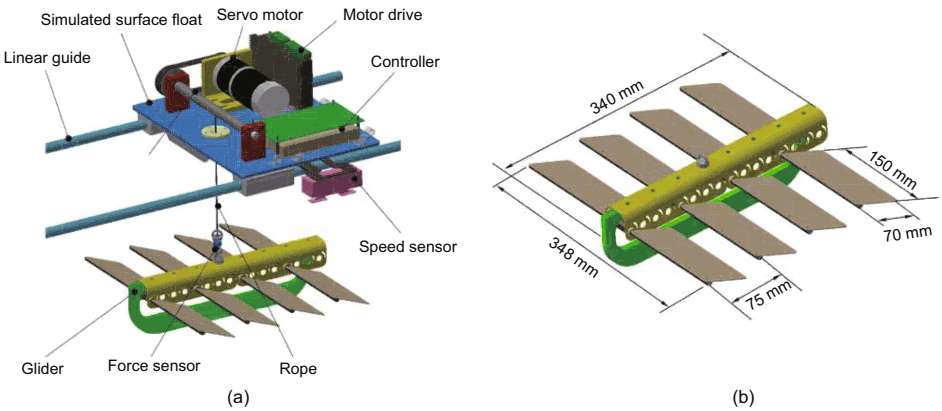

Fig. 8 Simulated vehicle testbed (a) (Simulated surface float moves on linear guides and the submerged glider moves under the control of a servo motor through a rope connection) and geometries of the glider (b)

glider drops due to its gravity. The glider pulls the surface float forward during this rhythmic pull-and-release. In this way, we can set different parameters to simulate the periodical ocean waves in the pool test by using Eq. (1). Because the sizes of the testing pool and the prototype are both limited, experiments have to be conducted in sea conditions lower than level 3. According to physical limitations, two types of wave are chosen as test samples in the experiments shown in Fig. 9. Fig. 10 shows the segments of the forward speeds in the simulation and the pool trial under wave height 0.21 m, period 2.2 s and wave height 0.24 m, period 2.0 s. The timer starts counting immediately once the glider moves. The first several periods of pull-release motion are discarded because the system's movement is not very stable at this stage. Thus, the time does not start at zero in Fig. 10. From the comparison, it can be concluded that the motion principle of the dynamic model is consistent largely with that of the platform. The average speed computed from the dynamic model is very similar to that of the platform. The relative error is within the range of 2%–10%. The nonlinear friction of the guide rail below the float and the inaccuracy of the drag coefficient in the simulation model may account for fluctuations of the speed curve in Fig. 10.

One large difference between this lab experiment setup and the true ocean environment is that the float in the lab testing cannot move vertically due to the constraints of the two linear guide rails and the fact that the length of the soft cable varies to simulate the wave motion, while on a real sea surface the float moves up and down with the ocean waves and the length of the soft cable remains unchanged. Fortunately, these two processes can be assumed equivalent because in the two cases the movements of the submerged glider are the same. The forward speed of the float comes from the motion of the glider. Therefore, in terms of forward movement, the two systems are equivalent. This explains why the speed peaks obtained in the experiments are much different from the theoretical ones in Fig. 10. However, the averaged forward speeds are approximately the same. This result could prove that the dynamic model is a useful tool for predicting the speed of the wave glider.

The forward speed is also influenced by the angle of attack of the glider wings. The propulsion of

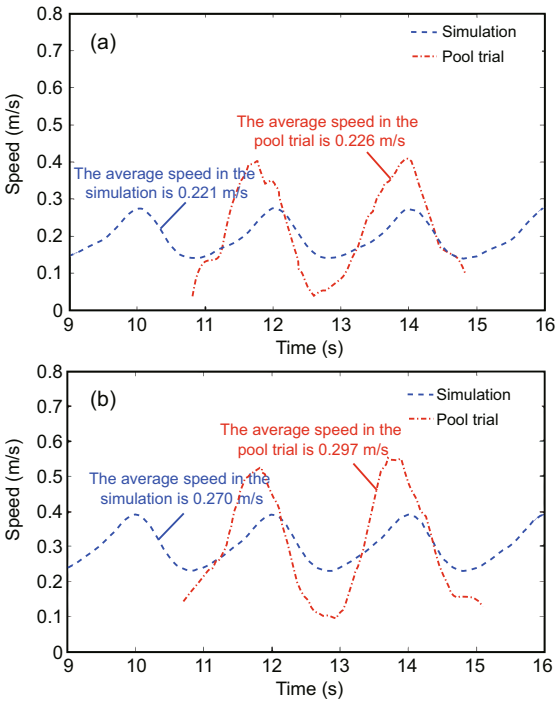

Fig. 10 Forward speeds in the simulation and pool trial under wave height 0.21 m (a) and 0.24 m (b)

the vehicle comes from the horizontal components of wing's drag force. A smaller angle of attack results in a smaller horizontal force; however, if the angel is too large, the total drag force will also be reduced. There is an optimal angle of attack yielding the largest forward propulsion force, as predicted by the dynamic model. In pool trials, several angles of attack are tested by manually tuning positions of wing stoppers. The forward speed curves under different angles are shown in Fig. 11, where two full wave periods of data are taken. It can be seen that there are obvious discrepancies in forward speeds with different angle settings. The average speeds are about 0.177, 0.263, 0.297, 0.351, and 0.323 m/s under 70°, 50°,

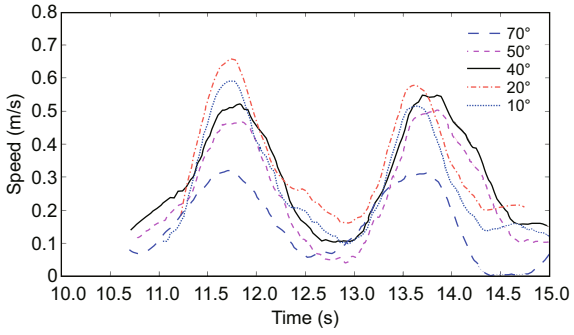

Fig. 11 Forward speeds under different angles of attack

40°, 20°, and 10°, respectively, which conforms to the optimal 20°–30° angle of attack deduced from the simulation. The influence of cable length on the forward speed is not investigated in the pool trial because of the limited depth of the pool.

5 Conclusions and future work

In this study, a dynamic model for the wave-propelled ASV, which can be incorporated with sea states to predict the forward speed of the wave-propelled vehicle, was established based on Kane's method. The validity of the model was demonstrated by simulation and pool trial to some extent. Key mechanism parameters of the vehicle were optimized with simulations of the dynamic model.

The actual ocean environment is very complex. Therefore, current research has to use experiment-based methods to predict the forward speed of the wave glider instead of an analytical model. The fundamental principle of a wave glider is that it converts up-down wave energy into forward moving energy. Although the ocean wave certainly contains many complex motions, we think that this up-down wave motion providing thrust for the wave glider is simple and can be modeled by math tools. Our study stands on this basis. The model is not dedicated to explaining all body-wave interaction processes, but focuses only on the relationship between forward speed and wave strength. In terms of speed prediction, the effectiveness of the model has been proven by lab pool trials. The first benefit from this model is that it gives us a tool for improving the mechanical design of the vehicle to enhance its performance. Another obvious benefit is that it provides us with a prior knowledge of the vehicle speed under different sea states. One can use the ocean forecast data to obtain the speed of the vehicle and thus make it possible to do path planning (Zhang *et al.*, 2016). Currently, the speed of the vehicle is difficult to predict. The experiment-based approaches may obtain a more accurate forward speed. The above benefits can hardly be obtained from them.

The accuracy of the model can be improved further. In the planning of future work, sensors like gyroscopes will be added to the float to measure real-time wave oscillations in field tests. By using actual wave data and on-board speed sensors on the float, the discrepancy between the predicted speed and the actual speed can be obtained, which is useful for improving the dynamic model. Incorporating numerical or experimental data to perform system identification is also a promising method for improving the model. If using such a method, a model structure should be obtained first. The dynamic model obtained in this study can play this role. The rest of the study would focus on how to regulate the parameters in the model. This is also an interesting topic worth investigating in our future study. The model will be expanded to a 3D model for control and path planning. We will also investigate the path planning problem for the wave-propelled vehicle considering dynamic ocean currents.

References

Caiti, A., Calabró, V., Grammatico, S., *et al.*, 2011. Lagrangian modeling of the underwater wave glider. MTS/IEEE Oceans, p.1-6. https://doi.org/10.1109/Oceans-Spain.2011.6003429

Cameron, S., 1994. Obstacle avoidance and path planning. *Ind. Robot*, **21**(5):9-14. https://doi.org/10.1108/EUM0000000004159

Carragher, P., Hine, G., Legh-Smith, P., *et al.*, 2013. A new platform for offshore exploration and production. *Oilfield Rev.*, **25**(4):40-50.

Cong, B., Cui, H.L., Liu, Z., 2009. Modeling and virtual simulation in random ocean waves. *J. Xi'an Technol. Univ.*, **29**(5):475-478 (in Chinese).

Daugherty, R.L., Franzini, J.B., 1997. Fluid Mechanics with Engineering Applications. McGraw-Hill, New York, p.192-198.

Hine, R., Willcox, S., Hine, G., *et al.*, 2009. The wave glider: a wave-powered autonomous marine vehicle. MTS/IEEE Oceans, p.1-6. https://doi.org/10.23919/OCEANS.2009.5422129

Kraus, N., Bingham, B., 2011. Estimation of wave glider dynamics for precise positioning. MTS/IEEE Oceans, p.1-9. https://doi.org/10.23919/OCEANS.2011.6107207

Liu, J.Y., Li, Y.H., Yi, H., *et al.*, 2011. The modeling and analysis of wave powering surface vehicle. MTS/IEEE Oceans, p.1-6. https://doi.org/10.23919/OCEANS.2011.6106971

Lolla, T., Ueckermann, M.P., Yiğit, K., *et al.*, 2012. Path planning in time dependent flow fields using level set methods. IEEE Int. Conf. on Robotics and Automation, p.166-173. https://doi.org/10.1109/ICRA.2012.6225364

Ma, X.F., Xu, X.R., Li, D.G., 1988. A recursive algorithm of robot dynamics based on the Kane's dynamical equation. *J. Beijing Univ. Iron Steel Technol.*, **10**(2):198-208 (in Chinese). https://doi.org/10.13374/j.issn1001-053x.1988.02.030

Manley, J., Hine, G., 2016. Unmanned surface vessels (USVs) as tow platforms: wave glider experience and results. MTS/IEEE Oceans, p.1-5 https://doi.org/10.1109/OCEANS.2016.7761234

Manley, J., Willcox, S., 2010. The wave glider: a new concept for deploying ocean instrumentation. *IEEE Instrum. Meas. Mag.*, **13**(6):8-13. https://doi.org/10.1109/MIM.2010.5669607

Ngo, P., Al-Sabban, W., Thomas, J., *et al.*, 2013. An analysis of regression models for predicting the speed of a wave glider autonomous surface vehicle. Proc. Australasian Conf. on Robotics and Automation, p.1-10.

Ngo, P., Das, J., Ogle, J., *et al.*, 2014. Predicting the speed of a wave glider autonomous surface vehicle from wave model data. IEEE/RSJ Int. Conf. on Intelligent Robots and Systems, p.2250-2256. https://doi.org/10.1109/IROS.2014.6942866

Smith, R.N., Das, J., Hine, G., *et al.*, 2011. Predicting wave glider speed from environmental measurements. MTS/IEEE Oceans, p.1-8. https://doi.org/10.23919/OCEANS.2011.6106989

Song, H., Zhang, J.H., Yang, P., *et al.*, 2016. Modeling of a dynamic dual-input dual-output fast steering mirror system. *Front. Inform. Technol. Electron. Eng.*, in press. https://doi.org/10.1631/FITEE.1601221

Tarn, T.J., Shoults, G.A., Yang, S.P., 1996. A dynamic model of an underwater vehicle with a robotic manipulator using Kane's method. *Auton. Robots*, **3**(2-3):269-283. https://doi.org/10.1007/BF00141159

Wiggins, S., Manley, J., Brager, E., *et al.*, 2010. Monitoring marine mammal acoustics using wave glider. MTS/IEEE Oceans, p.1-4. https://doi.org/10.1109/OCEANS.2010.5664537

Zhang, Y.W., Kieft, B., Rueda, C., *et al.*, 2016. Autonomous front tracking by a wave glider. MTS/IEEE Oceans, p.1-4. https://doi.org/10.1109/OCEANS.2016.7761070

Zhou, C.L., Low, K.H., 2014. On-line optimization of biomimetic undulatory swimming by an experiment-based approach. *J. Bion. Eng.*, **11**(2):213-225. https://doi.org/10.1016/S1672-6529(14)60042-1